International Journal of Nanomedicine

Dovepress
open access to scientific and medical research

Open Access Full Text Article

ORIGINAL RESEARCH

Delivery of a STING Agonist Using Lipid Nanoparticles Inhibits Pancreatic Cancer Growth

Sherin George Shaji[1], Pratikkumar Patel[1], Umar-Farouk Mamani[1], Yuhan Guo[1], Sushil Koirala[1], Chien-Yu Lin[1], Mohammed Alahmari[1], Evanthia Omoscharka[2], Kun Cheng[1]

[1]Division of Pharmacology and Pharmaceutical Sciences, School of Pharmacy, University of Missouri-Kansas City, Kansas City, MO, USA; [2]Department of Pathology, University Health/Truman Medical Center, School of Medicine, University of Missouri-Kansas City, Kansas, MO, USA

Correspondence: Kun Cheng, Email chengkun@umkc.edu

Introduction: The tumor microenvironment (TME) of pancreatic cancer is highly immunosuppressive and characterized by a large number of cancer-associated fibroblasts, myeloid-derived suppressor cells, and regulatory T cells. Stimulator of interferon genes (STING) is an endoplasmic reticulum receptor that plays a critical role in immunity. STING agonists have demonstrated the ability to inflame the TME, reduce tumor burden, and confer anti-tumor activity in mouse models. 2'3' cyclic guanosine monophosphate adenosine monophosphate (2'3'-cGAMP) is a high-affinity endogenous ligand of STING. However, delivering cGAMP to antigen-presenting cells and tumor cells within the cytosol remains challenging due to membrane impermeability and poor stability.

Methods: In this study, we encapsulated 2'3'-cGAMP in a lipid nanoparticle (cGAMP-LNP) designed for efficient cellular delivery. We assessed the properties of the nanoparticles using a series of in-vitro studies designed to evaluate their cellular uptake, cytosolic release, and minimal cytotoxicity. Furthermore, we examined the nanoparticle's anti-tumor effect in a syngeneic mouse model of pancreatic cancer.

Results: The lipid platform significantly increased the cellular uptake of 2'3'-cGAMP. cGAMP-LNP exhibited promising antitumor activity in the syngeneic mouse model of pancreatic cancer.

Discussion: The LNP platform shows promise for delivering exogenous 2'3'-cGAMP or its derivatives in cancer therapy.

Keywords: 2'3'-cGAMP, cold tumor, innate immunotherapy, lipid nanoparticle, cytosolic delivery

Introduction

Pancreatic cancer is the third leading cause of cancer-related death in the United States. It has the lowest 5-year relative survival rate of 12.5% compared to other types of cancer.[1] The most common type of pancreatic cancer is pancreatic adenocarcinoma (PDAC), which has a very poor prognosis and is predicted to become the second leading cause of cancer-related death in the US by 2030.[2] PDAC is characterized by the uncontrolled growth of exocrine cells in the pancreas and is predominantly classified as an immunologically cold tumor, with minimal infiltration of T cells. From a clinical perspective, the presence of T cell infiltration in the tumor microenvironment (TMC) of PDAC is associated with improved patient outcomes and longer survival.[3]

The stimulator of interferon genes (STING) is an endoplasmic reticulum membrane receptor that plays a crucial role in innate immunity.[4] The STING pathway is activated when viral, bacterial, tumoral or mitochondrial DNA is recognized by cyclic GMP-AMP synthase (cGAS). This recognition leads to the recruitment of 2'3'-cGAMP, which binds to the STING receptor.[5] Subsequently, the pathway induces a type-1 interferon (IFN) and chemokine response, followed by activation of both innate and adaptive immunity.[6] Numerous studies have demonstrated the benefits of STING pathway agonism in various types of cancer,[7–10] including pancreatic cancer in mouse models.[11,12] Cyclic dinucleotides (CDNs) can bind and activate the STING signaling pathway. In the mammalian innate immune system, the natural endogenous ligand, 2'3'-cGAMP which features a unique 2'-5' phosphodiester linkage, exhibits higher affinity than other CDNs.[13–15] In a proof-of-concept study, intratumoral administration of STING agonists demonstrated promising antitumor efficacy in

Received: 31 January 2024
Accepted: 19 July 2024
Published: 27 August 2024

mouse models by increasing the infiltration of $CD8^+$ T cells into tumors and effectively controlling tumor growth.[10] However, intratumoral drug administration is only feasible for a very limited number of cancer cases in clinical practice. Particularly, it cannot be used for metastatic tumors. In contrast, systemic administration is routinely employed in cancer therapy because drugs can reach both primary and metastatic tumor cells. Systemic administration of exogenous 2'3'-cGAMP faces challenges of poor stability, inefficient cellular uptake, and rapid clearance. Ectonucleotide pyrophosphatase/phosphodiesterase 1 (ENPP1), a hydrolase, can degrade extracellular 2'3'-cGAMP and attenuate the signaling of the STING pathway.[16,17] Moreover, 2'3'-cGAMP is a hydrophilic molecule with two negative charges, which hinder its cellular uptake.[17,18] Therefore, 2'3'-cGAMP alone cannot be administered systemically for therapeutic applications.

The delivery of active cargo using nano formulations present a promising strategy for PDAC therapy.[19,20] For example, Li utilized lipid nanoparticles containing a protamine-cGAMP complex to enhance the activation of the STING pathway in-vitro and suppressed the progression of melanoma in mouse models when combined with anti PD-L1 therapy.[21] However, these nanoparticles were injected directly into the tumor, whereas systemic administration is preferred for cancer therapy, especially for tumors that are inaccessible or metastatic. Our group recently discovered a novel biodegradable cationic lipid named LHHK. Through the modification of the lipid's headgroup with histidine or lysine, we screened a series of lipids and found that LHHK exhibited remarkable capability to deliver the *I-kappa-B kinase epsilon* (*IKBKE)* siRNA to cancer cells. This siRNA lipid nanoparticle (LNP) significantly inhibited tumor growth and demonstrated a favorable in-vivo safety profile.[22] Although the cellular internalization pathways of nanoparticles may differ based on its physical and chemical properties, the step of endosomal escape is critical to avoid degradation by lysosomes and deliver the encapsulated therapeutic cargo in the cytosol.[23] We predict that our amino-acid modified nanoparticles, composed of a cationic lipid with a pKa of 6.08,[22] would offer an advantage in this scenario by helping in the evasion of the lysosomal degradation and facilitating the release of 2'3'-cGAMP into the cytosol.

In our current study, we encapsulated 2'3'-cGAMP in the LHHK LNP to overcome the limitations associated with cGAMP degradation and to potentially achieve higher tumor accumulation. The objective of our study is to assess the properties of the nanoparticles using a series of in-vitro studies designed to evaluate their cellular uptake, cytosolic release, and minimal cytotoxicity. Furthermore, we examined the nanoparticle's anti-tumor effect in a syngeneic mouse model of pancreatic cancer.

Materials and Methods

Materials

2'3'-cGAMP (cat # B8362-5mg) was purchased from Apex Bio (Houston, TX) whereas 2',3'-cGAMP-Cy5 conjugate (# 20318) was ordered from AAT Bioquest Inc. (Pleasanton, CA). Float-A-Lyser G2 Dialysis device (G235031, cat # 08–607-021, MWCO 8–10 KDa) was bought from Fisher Scientific (Hampton, NH). Cell Titer-Glo luminescent cell viability assay kit (# G7570) and 2'3'-cGAMP ELISA Kit (# 501700) were purchased from Promega (Madison, WI) and Cayman Chemical (MI, USA), respectively. M-PER™ Mammalian Protein Extraction Reagent (# 78503) was bought from Thermo Fisher (Waltham, MA). THP1-Blue™ ISG Cells and Human Pancreatic Duct Epithelial Cell Line were bought from Invivogen (San Diego, CA) and Kerafast (Boston, MA), respectively. The Panc02 and DC2.4 cells were kindly provided by Dr. Gregory Lesinski (Emory University) and Dr. Kenneth Rock (University of Massachusetts Medical School), respectively. The NIH-3T3 cell line was purchased from American Type Culture Collection (Manassas, VA). Deidentified human whole blood (# HUMANWBK2-0000405) was purchased from BioIVT (Westbury, NY). All the cell lines and deidentified human whole blood have been approved by the Institutional Review Board (IRB) committee of the University of Missouri-Kansas City.

Cell Culture

Panc02 cells were cultured in Roswell Park Memorial Institute (RPMI) 1640 medium supplemented with 10% Fetal Bovine Serum, 1% penicillin, and 1% streptomycin. NIH-3T3 cells were cultured in Dulbecco's modified Eagle Medium (DMEM) supplemented with 10% Calf Bovine Serum, 1% penicillin, and 1% streptomycin. The Human Pancreatic Duct Epithelial Cells were cultured in Gibco™ Keratinocyte SFM medium (Cat# 17–005-042, Fisher Scientific) supplemented

with 1×antibiotic-antimycotic (Cat #15-240-062, Fisher Scientific). The DC2.4 cells were grown in RPMI-1640 supplemented with 10% FBS, 1% penicillin, 1% streptomycin, 2 mM L-glutamine, 50 μM 2-mercaptoethanol, 1× non-essential amino acid, and 10 mM HEPES. The THP1-Blue™ ISG cells were cultured according to the manufacturer's protocol. All cell lines were cultured in a humidified environment at 37°C with 5% CO_2.

Preparation and Characterization of cGAMP LNP

The cGAMP LNPs were prepared using a method we previously described, with some modifications.[22] Briefly, the ionizable lipid LHHK, Dipalmitoylphosphatidylcholine (DPPC), 1.2-Distearoyl-sn-glycero-3-phosphoethanolamine (DSPE)-mPEG$_{2000}$, and cholesterol at a molar ratio of 55:2:10:33 were dissolved in ethanol and mixed with 2.5 times volume of citrate buffer solution (pH 3, 50 mM) containing 2'3'-cGAMP to form the LNPs. The resulting mixture was then subjected to dialysis against PBS using a Float-A-Lyser G2 dialysis device (molecular weight cutoff 8–10 KDa) for 2 hours. The weight ratio of 2'3'-cGAMP to the ionizable lipid LHHK used in the LNP was 1:5. The particle size, polydispersity index (PDI) and zeta potential of the cGAMP-LNP were determined using a Malvern Zetasizer Nano ZS (Westborough, MA). The morphology of the nanoparticles was evaluated through transmission electron microscopy using a JEOL JEM- 1200 Ex II electron microscope.

Cellular Uptake Study

A total of 2×10^5 DC2.4 cells were seeded in a 12-well plate and incubated at 37°C in a CO_2 incubator for 16 hours. The medium was then discarded, and cells were washed twice with 1 mL of pre-warmed DPBS. Subsequently, cGAMP-LNP or 2'3'-cGAMP at final concentration of 0.5 μg/mL or 0.25 μg/mL of cGAMP in Opti-MEM™ was added to the respective wells. The plate was incubated for 2 hours at 37°C in a CO_2 incubator. The cells were then washed with DPBS, and 250 μL of cell lysis reagent (M-PER™ Mammalian Protein Extraction Reagent, Thermo scientific) was added to each well. The plate was then placed on an orbital shaker with a speed of 300 rpm for 5 minutes at room temperature to disrupt the cells. The cellular uptake was quantified using the 2'3'-cGAMP ELISA Kit (Cayman Chemical, MI, USA).

IRF Activation Study

To study the activation of interferon regulatory factor (IRF) in-vitro, 9×10^4 THP1-Blue™ ISG cells were incubated with different formulations in a flat bottom 96-well plate at 37°C for 24 hours. cGAMP-LNPs and 2',3'- cGAMP were added at final concentration of 0.5 μg/mL, 0.05 μg/mL, or 0.005 μg/mL of cGAMP. Blank LNP was prepared to match the lipid concentration of corresponding cGAMP-LNPs. After incubation, 20 μL of the supernatant from each well was transferred into a new 96-well plate containing 180 μL of QUANTI-Blue™ solution and incubated at 37°C for 4 hours. The levels of IRF-induced secreted embryonic alkaline phosphatase (SEAP) in the cell culture supernatant were determined by measuring absorbance at 655 nm using a SpectraMax 190 plate reader.

ex-vivo RBC Hemolysis Assay

The red blood cells (RBC) hemolysis assay was conducted according to a previously protocol to examine the endosomolytic activity of the LNPs.[24] Briefly, RBCs were isolated from the human blood, washed twice with a 150 nM NaCl (sodium chloride) solution, and then diluted at a ratio of 1:50 in a phosphate buffer with pH values of 5.6, 6.2, 6.8, or 7.4. Blank nanoparticles were incubated with the diluted RBC solution at appropriate pH in V-bottom 96-well plate (# 3894, Corning) at 37°C for an hour. The plate was then centrifuged at 1000×g for 5 minutes to pellet the RBCs. The supernatant was transferred to a new flat bottom 96-well plate, and the absorbance was measured at 405 nm. Cells treated with the corresponding pH phosphate buffer and 1% Triton X-100 were used as negative and positive controls, respectively, in the assay.

in vitro Cytotoxicity Assay

The cellular toxicity of cGAMP-LNP was evaluated using human pancreatic duct epithelial cells. Briefly, 1.5×10^4 cells were seeded in a 96-well plate with complete keratinocyte SFM medium and incubated for 24 hours at 37°C. The

medium was then removed, and different concentrations of cGAMP-LNP (5, 2.5, and 0.5 µg/mL) were added to each well. 1% Triton X-100 was used as positive control. The plate was further incubated for 24 hours at 37°C. Next, 200 µL of fresh medium and cell titer glo reagent at 1:1 (v/v) ratio were added to each well. The plate was placed on an orbital shaker (speed=300 rpm) for 7 minutes and then incubated at room temperature for 10 minutes. The luminescence was measured using a Spectramax ID5 plate reader.

Anti-Tumor Activity Study

The animal protocol was approved by the Institutional animal care and use committee (IACUC) of the University of Missouri-Kansas City in accordance with the Public Health Service's Policy on Humane Care and Use of Laboratory Animals, the Amended Animal Welfare Act of 1985, and the regulations of the United States Department of Agriculture (USDA). Equal number of male and female C57BL/6J (6 to 8-week-old) mice were used in animal studies. The body weight of mice was regularly measured at specified intervals. The mice were maintained in a pathogen-free environment within the temperature and humidity-controlled animal care facility on a 12-hour light-dark cycle.

C57BL/6J mice were subcutaneously implanted on the right flank with 50 µL of cell suspension containing a total of 1×10^6 cells (the mixture of Panc-02 and NIH-3T3 cells in a 2:1 ratio). Once tumors reached a volume of 100 mm^3, the mice were randomly divided into 4 groups (n=8) and received intraperitoneal administration with saline, cGAMP-LNP, free 2'3'-cGAMP, and blank LNP at dose of 1 mg/Kg on Days 8, 11, 14, and 17. The animal study was conducted in a blinded manner. One investigator injected the formulations to the mice, and another investigator monitored tumor growth without knowledge of the experimental groups. The dimensions of the tumors were recorded daily using a caliper, and the tumor volume (V) was calculated using the formula $V= (\text{length} \times \text{width}^2)/2$. At the end of the study (Day 22), the mice were euthanized, and all major organs including the heart, liver, lungs, kidney, spleen, and tumor were collected. The plasma samples were sent to the Veterinary Medical Diagnostic Laboratory at the University of Missouri for biochemical analysis.

Statistical Analysis

All the data were presented as mean±SD or SEM. For comparisons among more than two groups, Brown-Forsythe and Welch ANOVA or repeated measures one-way ANOVA was utilized along with Tukey's test for multiple comparisons. A p value of <0.05 was deemed statistically significant for all analysis.

Results

Preparation and Characterization of cGAMP-LNP

The cGAMP-LNP was prepared by using a 1:5 (w/w) ratio of 2'3'-cGAMP to ionizable lipid (LHHK) (Figure 1). Due to the enhanced permeability and retention (EPR) effect, nanoparticles in the size range of 100–200 nm accumulate in the tumor microenvironment.[25,26] The physical properties of the LNPs containing 2'3'-cGAMP were characterized using dynamic light scattering. The results showed that their hydrodynamic size ranged from 160–180 nm, with a polydispersity index (PDI) of less than 0.2 and a mean positive zeta potential of 11.1 (Figure 2a and b). Morphological evaluation using transmission electron microscopy (TEM) revealed that the LNPs had a spherical shape and a size below 200 nm (Figure 2c). Moreover, the pKa of LHHK is 6.08,[22] which facilitates efficient encapsulation of 2'3'-cGAMP at an acidic pH in the citrate buffer. The encapsulation efficiency of cGAMP-LNP on an average was found to be 75%.

cGAMP-LNP Displays an Enhanced IRF Activation

The in-vitro activity of cGAMP-LNP was evaluated using a monocytic reporter cell line, THP1-Blue™ ISG. This cell line is generated through stable integration of an IRF-inducible SEAP reporter construct. The level of SEAP is measured as an indicator of IRF activation in the cell line. IRF will be activated when cGAMP binds to STING. Therefore, this assay can be used to monitor the in vitro activity of 2'3'-cGAMP from the LNP. We found that cGAMP-LNP exhibited a higher level of activation compared to free cGAMP or blank LNP at the same concentration of cGAMP or lipid, respectively (Figure 3a). This also serves as evidence that the activation of the cell line is not solely attributable to cGAMP or lipid alone, but rather to

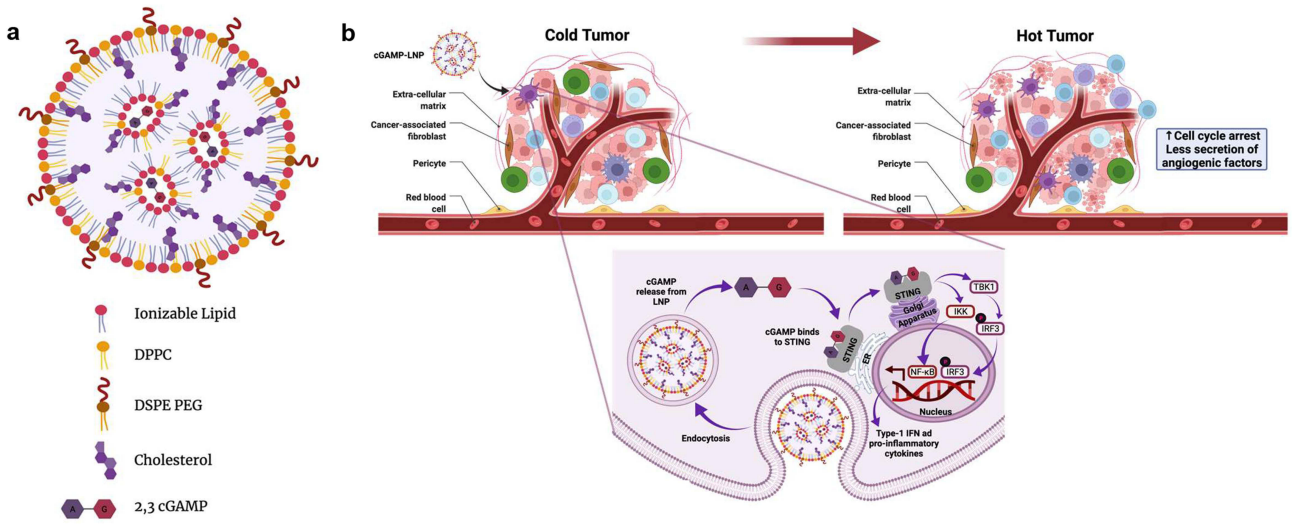

Figure 1 Schematics of cGAMP-LNP and its anti-tumor mechanism. (**a**) Schematics of the cGAMP-LNP (created using Biorender.com). (**b**) Anti-tumor mechanism of cGAMP-LNP.

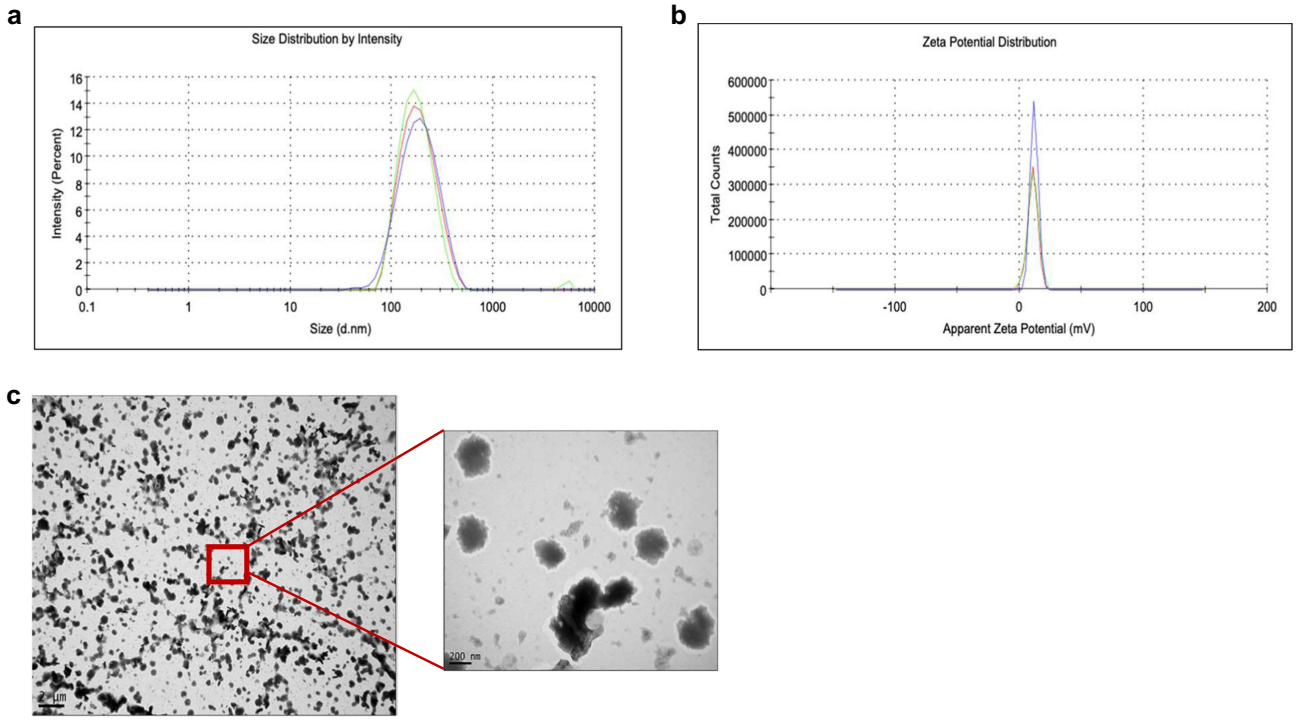

Figure 2 Characterization of cGAMP-LNPs. (**a**) Analysis of particle size using dynamic light scattering, (**b**) Zeta potential distribution, (**c**) Morphology was elucidated using TEM.

the effective encapsulation and delivery of cGAMP by the LNPs. Therefore, we determined the half maximal effective concentration (EC_{50}) of cGAMP-LNP and free cGAMP in THP1-Blue^{TM} ISG cells. We found that the EC_{50} for cGAMP-LNP was 105.5 nM (Figure 3b), whereas for free cGAMP, it was in micromolar range (3.04 μM) (Figure 3c).

Cellular Uptake and Cytotoxic Activity of cGAMP-LNP

We next examined the cellular uptake of cGAMP-LNP and free 2'3'-cGAMP (at cGAMP concentration of 0.5 and 0.25 μg/mL) in DC2.4 cells. The intracellular 2'3'-cGAMP concentration was measured using a 2'3'-cGAMP ELISA Kit

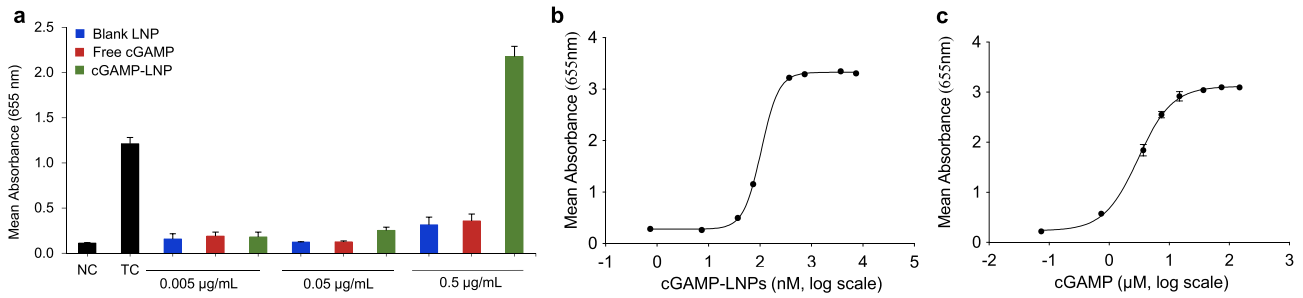

Figure 3 In-vitro activity of cGAMP-LNP. (**a**) IRF-inducible SEAP reporter activity of cGAMP LNP, blank LNP, and free 2'3'-cGAMP in THP-1 ISG reporter cell line. Poly (dA:DT)-Lyovec serves as a positive control. NC denotes negative control. (**b**) EC_{50} of the cGAMP-LNP. (**c**) EC_{50} of free 2'3'-cGAMP. All data are presented as mean ± SD (n=3).

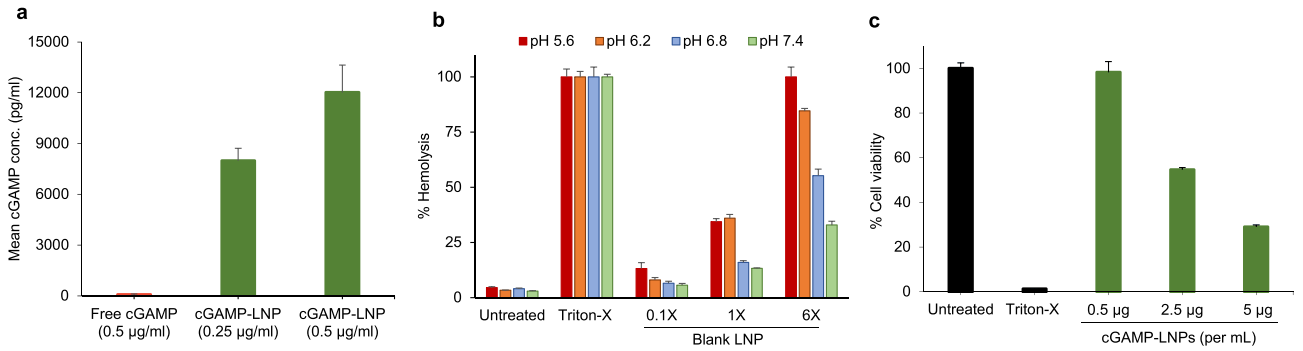

Figure 4 Cellular uptake, endosomolytic and cytotoxic activity of cGAMP-LNP. (**a**) Cellular uptake of cGAMP LNP and free cGAMP in DC2.4 cells. The DC2.4 cells were treated for 2 h with cGAMP-LNP or free cGAMP at cGAMP concentrations of 0.5 or 0.25 µg/mL, respectively. (**b**) The LNP induces pH- and concentration- dependent hemolysis of human RBCs. (**c**) Cytotoxicity of cGAMP-LNP in human pancreatic duct epithelial (HPDE) cells. All data are presented as mean ± SD (n=3).

following the manufacturer's protocol. The results confirmed the increased uptake of 2'3'-cGAMP by LNP at both concentrations (Figure 4a). In contrast, the presence of 2'3'-cGAMP within the cell treated with free 2'3'-cGAMP was either low or below the detection limit of the ELISA assay, which is consistent with a previous report.[7]

For 2'3'-cGAMP to bind to the STING receptor in the cytosol, cGAMP-LNP must escape the endo-lysosomal pathway and release the encapsulated 2'3'-cGAMP into the cytosol. Therefore, we investigated the endosomolytic activity of the blank LNP using an ex-vivo RBC hemolysis assay.[24] The blank LNP was prepared in a similar manner to cGAMP-LNP at concentrations of 6×, 1× and 0.1× of the lipid. The 0.1× blank LNP had the same lipid content as cGAMP-LNP at a 2'3'-cGAMP concentration of 0.5 µg/mL. When incubated with RBCs at different pH levels corresponding to physiological and endosomal compartments, the lipid displayed concentration- and pH-dependent endosomolytic activity (Figure 4b). Even at the highest lipid concentration, the blank LNP caused minimal disruption of RBCs at pH 7.4 but demonstrated robust hemolysis at the lower pH values associated with the late endo-lysosomal environment (pH 6.2 and pH 5.6). This result suggests that the LNP is safe for RBC in the bloodstream but capable of disrupting the endosome for efficient cytosolic drug delivery.

Moreover, we studied the impact of cGAMP-LNP on the cell viability of human pancreatic duct epithelial cells at 2'3'-cGAMP concentration of 0.5, 2.5 and 5 µg/mL. As illustrated in Figure 4c, the cells treated with cGAMP-LNP at 0.5 µg/mL exhibited a similar viability to the untreated group. However, at higher concentrations (2.5 and 5 µg/mL), the cell viability decreased. This decline could potentially be attributed to the high lipid content in the corresponding cGAMP-LNP formulations, and the lower number of cells initially seeded. In general, the cGAMP-LNP exhibited non-toxic properties, exhibited significant cellular uptake, and displayed favorable endosomolytic activity.

cGAMP-LNP Inhibits Tumor Growth in a Pancreatic Cancer Mouse Model

A subcutaneous pancreatic cancer mouse model was employed to assess the effect of cGAMP-LNP on tumor growth and development. One of the most prominent characteristics of PDAC is desmoplasia, the abundant fibrotic stroma, which comprises up to 80% of the tumor mass.[27,28] In the stromal microenvironment, activated pancreatic stellate cells (PSCs) transform from a quiescent state into a myofibroblast-like phenotype and produce a large amount of extracellular matrix (ECM) proteins, including collagens, fibronectins, and laminins. Therefore, to mimic human PDAC,[29] a mixture of NIH-3T3 fibroblast cells and Panc02 pancreatic cancer cells in a 1:2 ratio was utilized to generate the PDAC mouse model. All formulations were given intraperitoneally four times on day 8, 11, 14, and 17 with a 2'3'-cGAMP dose of 1 mg/Kg (Figure 5a). Across the treatment groups, no significant changes in body weight were observed (Figure 5b). Mice treated with cGAMP-LNP exhibited suppressed tumor growth when compared to saline, free 2'3'-cGAMP, and blank LNP (Figure 5c). These findings suggest that encapsulation of 2'3'-cGAMP within LNPs enhanced the therapeutic efficacy of 2'3'-cGAMP.

in-vivo Safety Profile of cGAMP-LNP

Keck and Muller proposed a nanotoxicological classification system (NCS) that categorizes nanosystems as no/low, medium or high risk based on their size and level of biodegradability.[30] Based on these criteria, cGAMP-LNP falls into the no or low-risk category because of their biodegradability and size above 100 nm. The biochemical analysis (Figure 6a) of various biomarkers assessed for potential toxicity in liver and kidney revealed that the mean values for all groups fell within the reference intervals previously reported for the C57BL/6J mouse strain.[31] Moreover, examination of H&E staining for the heart, kidney, liver, lung, and spleen specimens from different treatment groups showed similar morphology compared to the saline group (Figure 6b). Furthermore, these specimens were evaluated for inflammation on a scale of 0–5 (Figure 6c), and no significant difference was observed among the various treatments. Overall, the LNPs were determined to be non-toxic in-vivo.

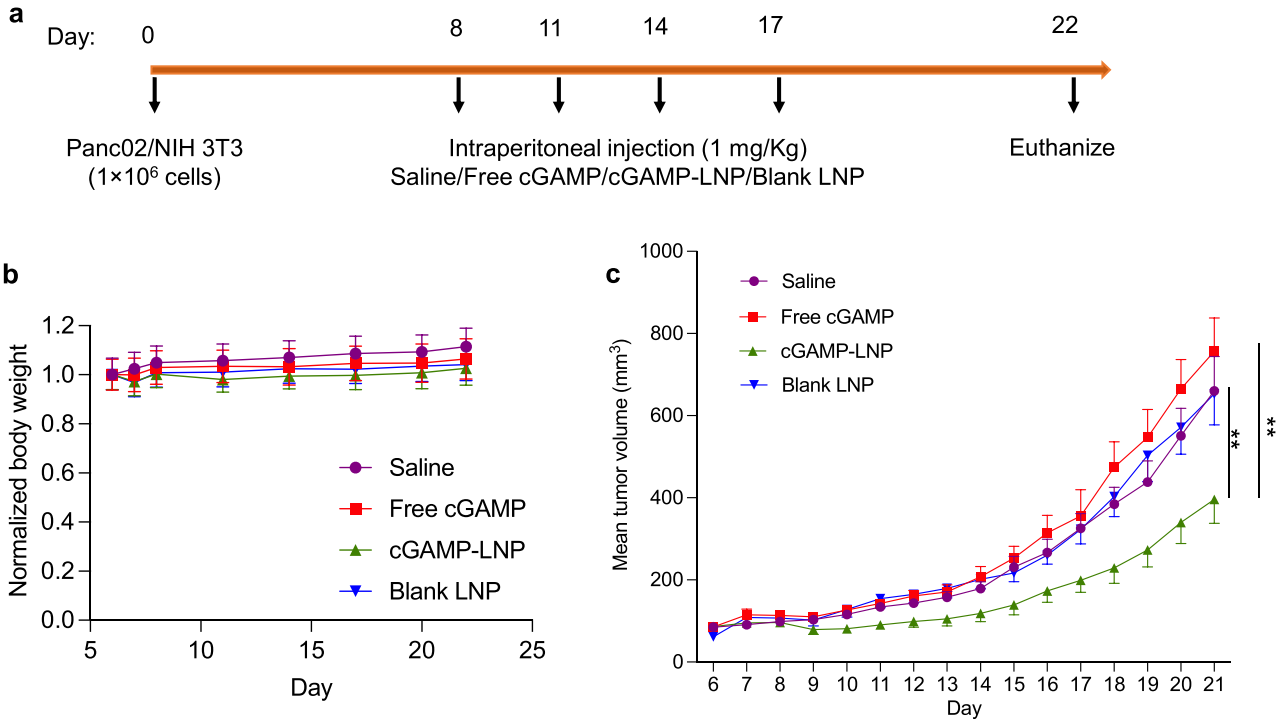

Figure 5 Anti-tumor activity of cGAMP-LNP in a mouse pancreatic cancer model. (**a**) C57BL/6 mice was implanted with a mixture of 1×10^6 Panc-02 and NIH-3T3 cells (2:1 ratio) subcutaneously on right flank. (**b**) Normalized body weight. (**c**) Tumor volume. Body weight was presented as mean ± SD (n=8). Tumor volumes were presented as mean ± SEM (n=8). $^{**}p<=0.005$.

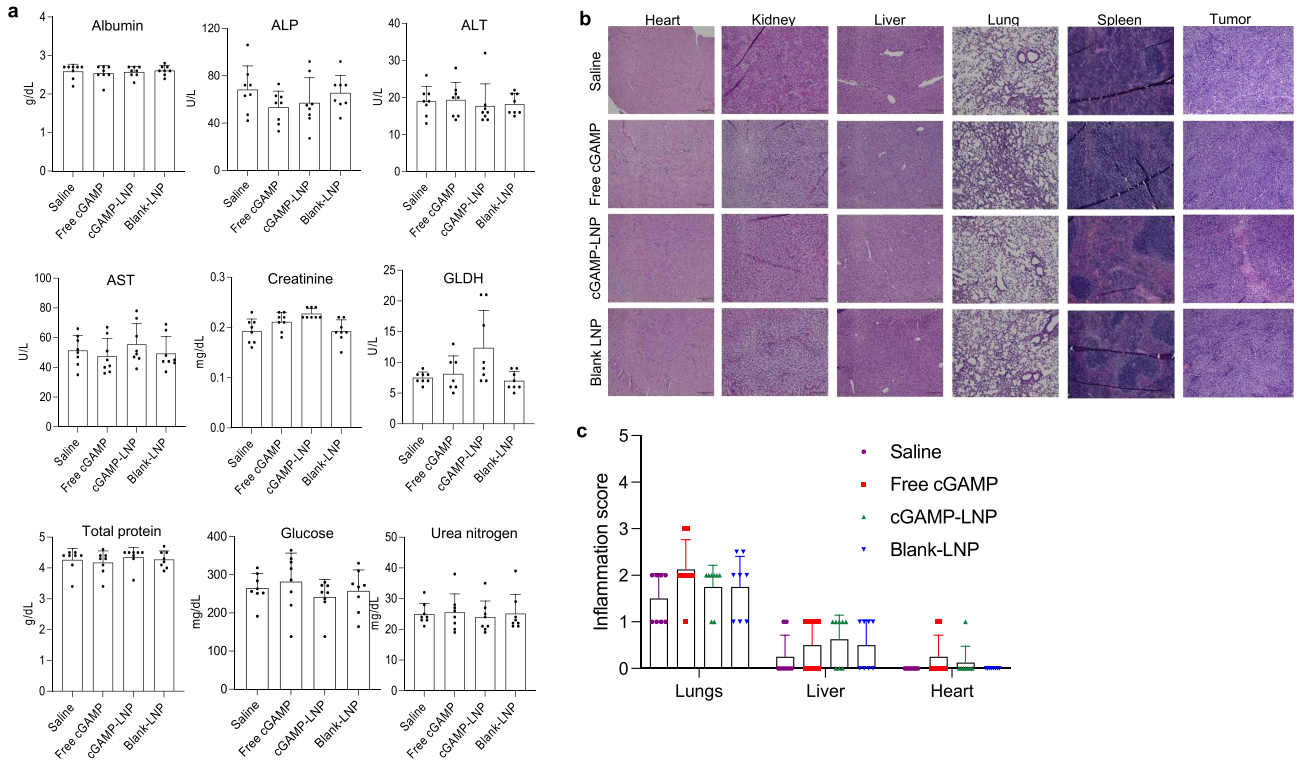

Figure 6 In-vivo toxicological evaluation of cGAMP-LNP. (**a**) Biochemical analysis levels of albumin, alkaline phosphatase (ALP), alanine transferase (ALT), aspartate aminotransferase (AST), creatinine, glutamate dehydrogenase (GLDH), total protein, glucose, and urea nitrogen in the plasma. (**b**) H&E staining of the heart, kidney, liver, lung, spleen, and tumor. The scale bar is 200 μm. (**c**) Inflammation score (scale of 0–5) of the lungs, liver, and heart. Kidney and spleen were reported to have no inflammation. The data were presented as mean ± SD (n=8).

Discussion

PDAC is the deadliest cancer with a very low 5-year survival rate. The challenges in treating PDAC arise from the lack of proper diagnostic tools to detect the cancer in early stages, as well as limited therapeutic options for advanced-stage cases. In addition, PDAC presents a highly immunosuppressive and difficult-to-penetrate TME,[29] which hampers the effectiveness of therapeutics. While checkpoint-based inhibitors have shown significant success in treating various types of cancer, only PD-1 therapy have demonstrated partial benefits for certain PDAC patients.[32,33]

Nanoparticles have been successfully employed as effective delivery systems for therapeutic or diagnostic agents in various diseases, including cancer. Recently, LNPs have gained significant attention due to their remarkable features, such as high encapsulation efficiency, biodegradability, non-toxicity, and ability to permeate cells.[26,34] Moreover, their physical properties, such as size, shape, surface characteristics, and drug release profiles can be modified to meet diverse requirements and overcome limitations in drug delivery.[25] We recently discovered a novel biodegradable cationic lipid named LHHK, which exhibited remarkable capability to deliver siRNAs to cancer cells. This siRNA LNP significantly inhibited tumor growth in a mouse cancer model and demonstrated a favorable in-vivo safety profile.[22] Because 2'3-cGAMP is negatively charged, we hypothesize that the same lipid can be used to encapsulate 2'3-cGAMP into LNP.

In this study, we aim to encapsulate 2'3-cGAMP into the LNP, increase its cellular uptake, and achieve maximum tumor accumulation while minimizing off-target responses. The preliminary characterization revealed that the size and zeta potential of the LNP provided an advantage over free 2'3'-cGAMP for efficient cytosolic delivery and release, resulting in a higher potential for IRF activation while being non-toxic to normal pancreatic cells at the same dose. In addition, encapsulation helped the cGAMP in the LNPs to remain protected and display potent in-vitro activity in the cell-based assay than free cGAMP. As our target receptor, STING, resides within the cytosol, we assessed the LNP's capability in a hemolysis assay to not only enter the cell but also efficiently escape endosome entrapment, avoid lysosomal degradation, and release cGAMP within the intracellular space. For this study, we used RBC as a surrogate

and incubated them with our LNPs in buffers mimicking endosomal and physiologic pH levels. We observed that our nanoparticles exhibited concentration- and pH-dependent endosomolytic activity. One potential challenge in using lipid-based carriers is the risk of organ toxicity, particularly in the liver and spleen. However, our cGAMP-LNP did not produce any significant toxic effect or inflammation in the major organs (Figure 6).

It is noteworthy to mention that we assessed the anti-tumor activity in a clinically relevant syngeneic PDAC mouse model by implanting a mixture of fibroblast cells and Panc02 pancreatic cancer cells. This model mimics the abundant fibrotic stroma found in PDAC tumors in human patients. This expanded fibrotic stroma and dysfunctional vasculature around PDAC tumors impede drug penetration and immune cell infiltration, leading to poor therapeutic efficacy.[35–37] Therefore, it is challenging to observe anti-tumor activity in this type of PDAC model. Despite these challenges, we observed significant anti-tumor activity with our LNP formulation after only four administrations using a 2'3'-cGAMP dose of 1 mg/kg (Figure 5). We believe that the anti-tumor activity will increase further if we administer additional doses of the LNP.

In conclusion, the LHHK cationic lipid, which was previously designed for siRNA, can also be employed to condense 2'3'-cGAMP into LNP. The cGAMP-LNP has improved the cellular uptake and tumor uptake of 2'3'-cGAMP, leading to encouraging anti-tumor activity in PDAC. The LNP platform holds promise for potential application in cancer therapy using exogenous 2'3'-cGAMP or its derivatives.

Acknowledgments

The work was supported by the National Institutes of Health (R01CA271592, R01CA231099, and R01GM121798) and a University of Missouri-Kansas City, School of Graduate Studies Research Award.

Disclosure

Kun Cheng reports a patent application for the lipids used in this article. The authors report no other conflicts of interest in this work.

References

1. Siegel RL, Miller KD, Wagle NS, Jemal A. Cancer Statistics, 2023. *CA Cancer J Clin*. 2023;73(1):17–48. doi:10.3322/caac.21763
2. R L, S BD, A R, R AB, F JM, M LM. Projecting cancer incidence and deaths to 2030: the unexpected burden of thyroid, liver, and pancreas cancers in the United States. *Cancer Res*. 2014;74(11):2913–2921. doi:10.1158/0008-5472.CAN-14-0155
3. Huber M, Brehm CU, Gress TM, et al. The immune microenvironment in pancreatic cancer. *Int J Mol Sci*. 2020;21(19):7307. doi:10.3390/ijms21197307
4. Ishikawa H, Barber GN. STING an endoplasmic reticulum adaptor that facilitates innate immune signaling. *Nature*. 2008;455:7213):674–8. doi:10.1038/nature07317
5. Zhang X, Shi H, Wu J, et al. Cyclic GMP-AMP containing mixed phosphodiester linkages is an endogenous high-affinity ligand for STING. *Mol Cell*. 2013;51(2):226–235. doi:10.1016/j.molcel.2013.05.022
6. W H, H S, C X, et al. cGAS is essential for the antitumor effect of immune checkpoint blockade. *Proceedings of the National Academy of Sciences of the United States of America*. 2017;114(7). doi:10.1073/pnas.1621363114
7. Shae D, Becker KW, Christov P, et al. Endosomolytic polymersomes increase the activity of cyclic dinucleotide sting agonists to enhance cancer immunotherapy. OriginalPaper. *Nat Nanotechnol*. 2019;14(3):269–278. doi:10.1038/s41565-018-0342-5
8. Liu Y, Crowe WN, Wang L. An inhalable nanoparticulate STING agonist synergizes with radiotherapy to confer long-term control of lung metastases. *Nature Communications*. 2019;10(1):5108. doi:10.1038/s41467-019-13094-5
9. Flood BA, Higgs EF, Li S, Luke JJ, Gajewski TF. STING pathway agonism as a cancer therapeutic. *Immunol Rev*. 2019;290(1):24–38. doi:10.1111/imr.12765
10. Corrales L, Glickman Laura H, McWhirter Sarah M, et al. Direct activation of STING in the tumor microenvironment leads to potent and systemic tumor regression and immunity. *Cell Rep*. 2015;11(7):1018–1030. doi:10.1016/j.celrep.2015.04.031
11. Jing W, McAllister D, Vonderhaar E, et al. STING agonist inflames the pancreatic cancer immune microenvironment and reduces tumor burden in mouse models. *J Immunother Cancer*. 2019;7(1):115. doi:10.1186/s40425-019-0573-5
12. Vonderhaar EP, Barnekow NS, McAllister D, et al. STING activated tumor-intrinsic type i interferon signaling promotes CXCR3 dependent antitumor immunity in pancreatic cancer. *Cell Mol Gastroenterol Hepatol*. 2021;12(1):41–58. doi:10.1016/j.jcmgh.2021.01.018
13. Wu J, Sun L, Chen X, et al. Cyclic GMP-AMP is an endogenous second messenger in innate immune signaling by cytosolic DNA. *Science*. 2013;339(6121):826–830. doi:10.1126/science.1229963
14. Danilchanka O, Mekalanos JJ. Cyclic dinucleotides and the innate immune response. *Cell*. 2013;154(5):962–970. doi:10.1016/j.cell.2013.08.014
15. Kalia D, Merey G, Nakayama S, et al. Nucleotide, c-di-GMP, c-di-AMP, cGMP, cAMP, (p)ppGpp signaling in bacteria and implications in pathogenesis. *Chem Soc Rev*. 2013;42(1):305–341. doi:10.1039/c2cs35206k
16. Carozza JA, Böhnert V, Nguyen KC, et al. Extracellular cGAMP is a cancer-cell-produced immunotransmitter involved in radiation-induced anticancer immunity. *Nat Cancer*. 2020;1(2):184–196. doi:10.1038/s43018-020-0028-4

17. Li L, Yin Q, Kuss P, et al. Hydrolysis of 2′3′-cGAMP by ENPP1 and design of nonhydrolyzable analogs. OriginalPaper. *Nat Chem Biol*. 2014;10(12):1043–1048. doi:10.1038/nchembio.1661
18. Dane EL, Belessiotis-Richards A, Backlund C, et al. STING agonist delivery by tumour-penetrating PEG-lipid nanodiscs primes robust anticancer immunity. *Nat Mater*. 2022;21(6):710–720. doi:10.1038/s41563-022-01251-z
19. Li Y, Zhao Z, Lin CY, et al. Silencing PCBP2 normalizes desmoplastic stroma and improves the antitumor activity of chemotherapy in pancreatic cancer. *Theranostics*. 2021;11(5):2182–2200. doi:10.7150/thno.53102
20. Li Y, Zhao Z, Liu H, et al. Development of a tumor-responsive nanopolyplex targeting pancreatic cancer cells and stroma. *ACS Appl Mater Interfaces*. 2019;11(49):45390–45403. doi:10.1021/acsami.9b15116
21. Li K, Ye Y, Liu L, et al. The Lipid platform increases the activity of STING agonists to synergize checkpoint blockade therapy against melanoma. *Biomater Sci*. 2021;9(3):765–773. doi:10.1039/D0BM00870B
22. Patel P, Fetse J, Lin C-Y, et al. Development of amino acid-modified biodegradable lipid nanoparticles for siRNA delivery. *Acta Biomater*. 2022;154:374–384. doi:10.1016/j.actbio.2022.09.065
23. Liu CG, Han YH, Kankala RK, Wang SB, Chen AZ. Subcellular performance of nanoparticles in cancer therapy. *Int J Nanomedicine*. 2020;15:675–704. doi:10.2147/ijn.S226186
24. Evans BC, Nelson CE, Yu SS, et al. Ex vivo red blood cell hemolysis assay for the evaluation of pH-responsive endosomolytic agents for cytosolic delivery of biomacromolecular drugs. *J Vis Exp*. 2013;(73):e50166. doi:10.3791/50166
25. Petros RA, DeSimone JM. Strategies in the design of nanoparticles for therapeutic applications. *Nature Reviews Drug Discovery*. 2010;9(8):615–627. doi:10.1038/nrd2591
26. Scioli Montoto S, Muraca G, Ruiz ME. Solid lipid nanoparticles for drug delivery: pharmacological and biopharmaceutical aspects. Review. *Front Mol Biosci*. 2020;7. doi:10.3389/fmolb.2020.587997
27. Erkan M, Hausmann S, Michalski CW, et al. The role of stroma in pancreatic cancer: diagnostic and therapeutic implications. *Nat Rev Gastroenterol Hepatol*. 2012;9(8):454–467. doi:10.1038/nrgastro.2012.115
28. Apte MV, Wilson JS, Lugea A, Pandol SJ. A starring role for stellate cells in the pancreatic cancer microenvironment. *Gastroenterology*. 2013;144(6):1210–1219. doi:10.1053/j.gastro.2012.11.037
29. Karamitopoulou E. The tumor microenvironment of pancreatic cancer. *Cancers*. 2020;12(10):3076. doi:10.3390/cancers12103076
30. Keck CM, Müller RH. Nanotoxicological classification system (NCS) – a guide for the risk-benefit assessment of nanoparticulate drug delivery systems. *Eur J Pharm Biopharm*. 2013;84(3):445–448. doi:10.1016/j.ejpb.2013.01.001
31. Stahl FR, Jung R, Jazbutyte V, et al. Laboratory diagnostics of murine blood for detection of mouse cytomegalovirus (MCMV)-induced hepatitis. *Sci Rep*. 2018;8(1):14823. doi:10.1038/s41598-018-33167-7
32. Yoon JH, Jung Y-J, Moon S-H. Immunotherapy for Pancreatic Cancer. *World J Clin Cases*. 2021;9(13):2969–2982. doi:10.12998/wjcc.v9.i13.2969
33. H-B L, Yang Z-H, Guo -Q-Q. Immune checkpoint inhibition for pancreatic ductal adenocarcinoma: limitations and prospects: a systematic review. *Cell Commun Signal*. 2021;19(1):117. doi:10.1186/s12964-021-00789-w
34. Patel P, Ibrahim NM, Cheng K. The importance of apparent pka in the development of nanoparticles encapsulating siRNA and mRNA. *Trends Pharmacol Sci*. 2021;42(6):448–460. doi:10.1016/j.tips.2021.03.002
35. Kota J, Hancock J, Kwon J, Korc M. Pancreatic cancer: stroma and its current and emerging targeted therapies. *Cancer Lett*. 2017;391:38–49. doi:10.1016/j.canlet.2016.12.035
36. Whatcott CJ, Diep CH, Jiang P, et al. Desmoplasia in primary tumors and metastatic lesions of pancreatic cancer. *Clin Cancer Res*. 2015;21(15):3561–3568. doi:10.1158/1078-0432.CCR-14-1051
37. Olive KP, Jacobetz MA, Davidson CJ, et al. Inhibition of Hedgehog signaling enhances delivery of chemotherapy in a mouse model of pancreatic cancer. *Science*. 2009;324(5933):1457–1461. doi:10.1126/science.1171362